ACS chemical biology

Articles

pubs.acs.org/acschemicalbiology

# Two-Color 810 nm STED Nanoscopy of Living Cells with Endogenous SNAP-Tagged Fusion Proteins

Alexey N. Butkevich,[†,∥] Haisen Ta,[†,∥] Michael Ratz,[†,§] Stefan Stoldt,[†] Stefan Jakobs,*[,†,‡] Vladimir N. Belov,*[,†] and Stefan W. Hell*[,†]

[†]Department of NanoBiophotonics, Max-Planck Institute for Biophysical Chemistry, Am Fassberg 11, 37077 Göttingen, Germany
[‡]Department of Neurology, University of Göttingen Medical Faculty, Robert-Koch-Str. 40, 37075 Göttingen, Germany

Supporting Information

**ABSTRACT:** A 810 nm STED nanoscopy setup and an appropriate combination of two fluorescent dyes (Si-rhodamine *680SiR* and carbopyronine *610CP*) have been developed for near-IR live-cell super-resolution imaging. Vimentin endogenously tagged using the CRISPR/Cas9 approach with the SNAP tag, together with a noncovalent tubulin label, provided reliable and cell-to-cell reproducible dual-color confocal and STED imaging of the cytoskeleton in living cells.

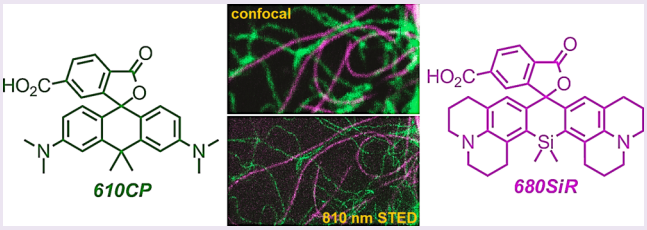




The current live-cell STED microscopy with synthetic fluorophores typically relies on the use of overexpressed target proteins fused to a protein tag.[1] Plasmid-driven overexpression may introduce numerous imaging artifacts including protein mislocalization and/or aggregation,[2] often hampering the interpretation of such experiments. Endogeneous tagging of mammalian proteins by CRISPR/Cas9 mediated genome editing[3,4] may alleviate these problems and has been highly beneficial for fluorescent protein-based RESOLFT live cell nanoscopy.[5] In this report, we use CRISPR/Cas9 to generate a mammalian cell line that expresses vimentin-SNAP, label it with a new far-red emitting dye *680SiR*, and image with a lower phototoxicity[6] using a 810 nm de-excitation beam.

In early reports on two-color live-cell STED microscopy with synthetic organic fluorophores, the staining of CLIP or SNAP fusion proteins was realized with commercially available dyes, *e.g.*, Atto 647N and Chromeo494.[7] The commercial STED microscopes offer a powerful pulsed 775 nm STED laser, and *SiR* dye[8] (Figure 1), as well as several other cell-permeant rhodamines and carborhodamines[9−12] with suitable emission profiles, have been developed and employed in two-color STED imaging of living cells. Most recently, two-color STED microscopy has been extended into the IR region by using an 810 nm STED beam and a pair of NIR-emitting Si-rhodamine labels (*SiR* and *SiR700*, see Figure 1).[13] The near-infrared spectral region (NIR or IR-A, 700−1400 nm) is attractive for deep tissue and *in vivo* optical imaging. Due to reduced background autofluorescence from biomolecules, photons at longer wavelengths provide higher contrast between the objects of interest and the background and penetrate deeper into living tissue.[14] In practice, however, the absorption and emission maxima of fluorophores have been confined within 650−900

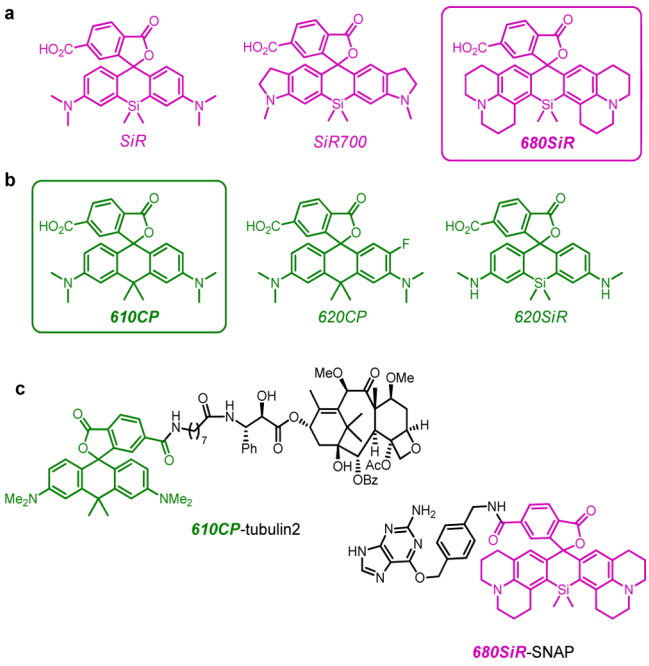


**Figure 1.** (a) Structures of *SiR*, *SiR700*, and *680SiR*, a novel rigidized *SiR* analog. (b) Structures of cell-permeant dyes suitable for the complementary color in two-color 810 nm STED microscopy. (c) Structures of the probes used for two-color STED imaging.

**Special Issue:** Chemical Biology of CRISPR

**Received:** July 21, 2017
**Accepted:** September 21, 2017
**Published:** September 21, 2017




DOI: 10.1021/acschembio.7b00616
*ACS Chem. Biol.* 2018, 13, 475−480

nm limits due to lower detector sensitivity above 900 nm and sample absorption bands at >950 nm.

The selection of a NIR-emitting fluorescent probe remains critical for many NIR bioimaging applications.[15] The most widely used NIR dyes are cyanines, having high extinction coefficients (typically $\varepsilon > 10^5$ $M^{-1}$ $cm^{-1}$), but they suffer from low photostability.[16] Porphyrins, phthalocyanins, and related polycyclic dyes have excellent photostabilities, and their emission easily reaches the NIR region. However, these large flat molecules have high molecular masses and low solubility in aqueous media. In addition, they show significant phototoxicity upon excitation—an effect that has found its use in photodynamic therapy.[17] Squaraine dyes have very high extinction coefficients ($\varepsilon$ up to $2-3 \times 10^5$ $M^{-1}$ $cm^{-1}$), but they are less photostable than triarylmethane dyes, undergo facile nucleophilic addition of thiols (e.g., glutathione in living cells), and readily form nonfluorescent aggregates in polar media.[18]

Among the newest developments, Si-rosamine-derived dyes,[19] Ge-rhodamines,[20] sulfone-rosamines,[21] and phosphorosamines[22] (e.g., Nebraska Reds, $\varepsilon$ up to $1.7 \times 10^5$ $M^{-1}$ $cm^{-1}$) represent fluorophores applicable in living cells. From these classes, successful generation of a cell membrane permeable probe has been achieved only with Ge-rhodamines and Si-rhodamine *SiR700* (Figure 1; SNAP-tag, F-actin, $\beta$-tubulin, and cathepsin D ligands were reported).[13] All NIR-emitting triarylmethane dyes with $>SiR_2$,[19] $>GeR_2$,[20] $>SO_2$,[21] or $>P(O)R$[22] bridges show modest fluorescence quantum yields ($\leq$0.4), especially in aqueous buffers. Incorporation of nitrogen atoms of fluorophores into azetidinyl groups increases the emission efficiency, and it has recently been proposed for several classes of dyes.[23] The suggested mechanism is a suppression of the transition into a TICT (twisted internal charge transfer) state, considered as a major contributor to nonradiative decay of excited fluorophore molecules. However, while this modification improves molecular brightness by a factor of 4–19.2 for coumarin dyes, 2.3-fold for acridines, 2.8-fold for rhodamines, 4-fold for rhodols, and 3.1-fold for oxazines, only a 5% increase was observed for a sample carborhodamine and 42% for a Si-rhodamine[23] (calculated as $(\varepsilon\Phi)/(\varepsilon_0\Phi_0)$, where $\varepsilon$ and $\varepsilon_0$ and $\Phi$ and $\Phi_0$ are extinction coefficients and fluorescence quantum yields for an azetidine-containing dye and its dialkylamino analog, respectively, measured under identical conditions). An attempt to extend the emission of Si-rhodamines to 700 nm and beyond by fluorination of the *SiR* core led to compounds with a high content of the nonfluorescent lactone form.[9]

An alternative way of suppressing the TICT and improving the brightness of a triarylmethane dye is based on blocking the rotation of the dialkylamino groups by their inclusion within a conformationally rigid julolidine or tetrahydroquinoline core. For example, replacement of two diethylamino groups in rhodamine B with julolidine cycles in rhodamine 101 results in nearly 3-fold improvement of the fluorescence quantum yield ($\Phi$ = 0.36 vs 0.99) and an increase in the lifetime from 1.75 to 4.91 ns in water.[24] This promising observation prompted us to synthesize a bis-julolidine-fused analog of *SiR* dye, *680SiR* (Figure 1 and Scheme 1).

## RESULTS AND DISCUSSION

**Synthesis of *680SiR* Dye.** 8-Bromojulolidine **1** was converted into a symmetrical diarylmethane **2**, and the latter was transformed into the reactive blue silaxanthylium dye **3** in a one-pot procedure. Bis-orthoester **4**-Br (prepared from bromoterephthalic acid) was subjected to bromine–lithium exchange, and the precursor dye **3** was added at −78 °C to the excess of aryllithium reagent **4**-Li. The intermediate leuco-dye (not isolated) was oxidized with DDQ, and the protecting ester groups were removed upon treatment with lithium hydroxide (see Supporting Information).[25] Use of a cationic precursor (a xanthylium salt of type **3**) was critical, as the reaction of the aryllithium reagent with the corresponding electron-rich benzophenone failed to provide the desired triarylmethane. The proposed approach may also be extended to the preparation of other rhodamine analogs (carbo- or germanorhodamines with policyclic structures). The photophysical properties of *680SiR* and related dyes (Figure 1) are given in Table 1 and Figures S1 and S2 (Supporting Information).

**Scheme 1. Synthesis of NIR Fluorescent Si-Rhodamine Dye *680SiR* (DDQ = 2,3-Dichloro-5,6-dicyano-1,4-benzoquinone)**

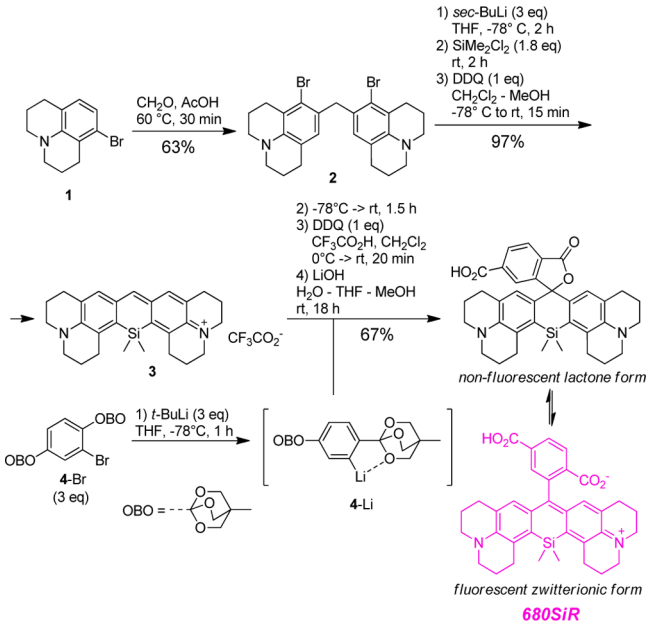


**Endogenous Tagging of Vimentin.** In previous work, selective labeling of vimentin in living cells with small molecule fluorophores was realized with overexpression employing vimentin-HaloTag fusion protein[9,20] or genetic code expansion.[26] To facilitate robustness and reproducibility of *in vivo* labeling, we have generated human knock-in cell lines expressing SNAP- or Halo-tagged vimentin from its genomic locus using the CRISPR approach.[4] To this end, human U2OS cells were cotransfected with a plasmid encoding Cas9/gRNA together with a vimentin-SNAP or vimentin-Halo donor plasmid.[5] Successfully targeted vimentin-SNAP or vimentin-Halo knock-in cells were identified by incubation with *SiR*-SNAP or *SiR*-Halo,[8] respectively, and individual cells were FACS-sorted into 96-well plates. Monoclonal cell lines that expressed the vimentin-SNAP or vimentin-Halo fusion protein as determined by fluorescence microscopy were kept in culture and verified by immunoblotting for transgene expression (Figure 2A and B). All cell lines obtained were heterozygous for the respective transgene.

**A Single-Laser 810 nm STED Nanoscopy Setup.** For testing the performance of the new dye (*680SiR*) in super-resolution microscopy, a home-built two-color NIR STED setup was designed for live-cell imaging (Figure S3). A single Ti:sapphire 810 nm laser was used for both single- and two-



DOI: 10.1021/acschembio.7b00616
ACS Chem. Biol. 2018, 13, 475–480

**Table 1. Properties of the Dyes Used in the Current Study, *SiR* and *SiR700* (in Aqueous PBS, pH 7.4)[a]**

| dye | absorption $\lambda_{max}$ [nm] ($\varepsilon$ [$M^{-1}cm^{-1}$], $\times 10^5$) | emission $\lambda_{max}$ [nm] ($\Phi_{fl}$) | brightness relative to *SiR* | $D_{0.5}$ | fluorescence lifetime $\tau$ [ns] |
|---|---|---|---|---|---|
| ***610CP*** | **609 (1.00)** | **634 (0.59)** | **1.63** | **36** | **3.1** |
| *620CP* | 617 (0.73) | 647 (0.17) | 0.33 | 63 | 1.0 |
| *620SiR* | 617 (0.80) | 638 (0.49) | 1.03 | 67 | 3.0 |
| *SiR*[8,9] | *645 (0.93)* | *661 (0.41)* | 1 (ref.) | 65 | 2.7 |
| ***680SiR*** | **679 (0.86)** | **697 (0.42)** | **0.95** | **24** | **3.0** |
| *SiR700*[13] | 689 (1.00) | 716 (0.13) | 0.13 | 59 | 1.4 |

[a]All dyes were used as 6′-carboxy isomers. Brightness relative to *SiR*: $(\varepsilon \times \Phi_{fl})_{dye}/(\varepsilon \times \Phi_{fl})_{SiR}$; $D_{0.5}$ is defined as an interpolated dielectric constant of 1,4-dioxane/water mixture, at which the normalized absorption of the dye is equal to one half the maximal value observed across the entire dioxane/water gradient (Figure S2).[9] For the absorption and emission spectra of the new dyes *620SiR* and *680SiR*, see Figure S1.

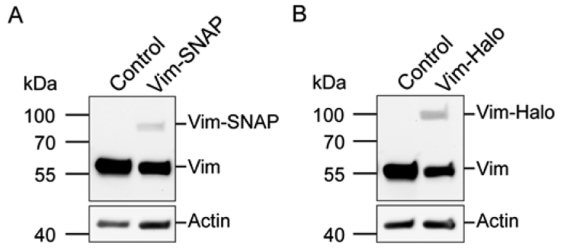


**Figure 2.** CRISPR/Cas9 mediated tagging of vimentin (Vim) with SNAP or Halo tags. Western blots of cell lysates of monoclonal heterozygous cells. Blots were decorated with antibodies against the SNAP tag (A) or the Halo tag (B). Loading control: actin antibody.

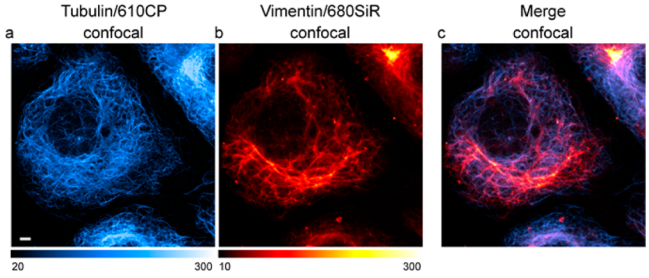


**Figure 4.** Confocal images of Vim-SNAP knock-in cells labeled with *610CP*-tubulin2 and *680SiR*-SNAP probes acquired using a Leica TCS SP8 beam scanning confocal microscope (a–c). Except for Lagrange interpolation and contrast stretching, no further image processing was applied. Scale bar: 5 $\mu$m (a–c).

color super-resolution imaging (Figure 3). To this end, the *p*-polarization light from the laser was fed into a crystal fiber to generate white light. Then, it was split with a dichroic mirror into two confocal excitation channels (610/10 nm and 670/10 nm). To increase the pulse duration of the STED (810 nm) beam from the femtosecond into the picosecond range, the short laser pulses were coupled into a long (110 m) fiber, providing ~120 ps pulses at the sample. A 2 Pi wave plate was utilized in the STED beam for the generation of a donut-shaped STED beam (with zero intensity at the center of the excitation focal spot). Scanning over the sample was realized with an original quartz beam scanner (QS).

**Dye Properties and Microscopy.** The near-IR emitting dye *680SiR* demonstrates ~35 nm bathochromic and bathofluoric shifts compared to the parent *SiR* and higher preference for the fluorescent zwitterionic form in the equilibrium (lower $D_{0.5}$ values in Figure S2, higher content of the fluorescent form).[9] In spite of this considerable red shift, the fluorescence quantum yield, extinction coefficient, and fluorescence lifetime of *680SiR* in neutral aqueous buffer are as high as those of *SiR*. The data in Table 1 demonstrate that *680SiR* is a brighter dye than *SiR700*,[13] where brightness is defined as a product of the fluorescence quantum yield and the molar extinction coefficient. Brighter dyes are easier to detect as they provide higher signal-to-noise ratio. The excited state lifetimes of *680SiR* and *SiR700* are 3.0 and 1.4 ns, respectively. The emission signals of these dyes can be separated by recording fluorescence lifetime, and thus this pair represents two complementary dyes for far-red superresolution imaging.[27] Similarly to the commercially available *SiR700*-$C_8$ label (Spirochrome) and unlike the original *SiR*, the conjugate of *680SiR* with BG-amine (SNAP-tag ligand; see Figure 1) did not demonstrate a significant increase in fluorescence upon binding to the SNAP-tag protein. The observed fluorogenic response

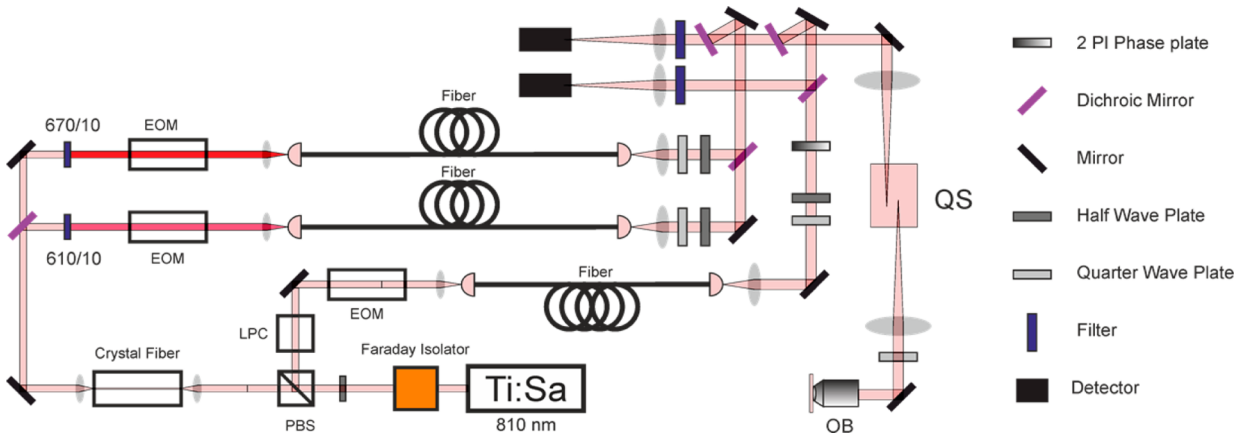


**Figure 3.** Two-color NIR STED setup used for live-cell imaging (see text and Supporting Information for the detailed description).



DOI: 10.1021/acschembio.7b00616
*ACS Chem. Biol.* 2018, 13, 475–480

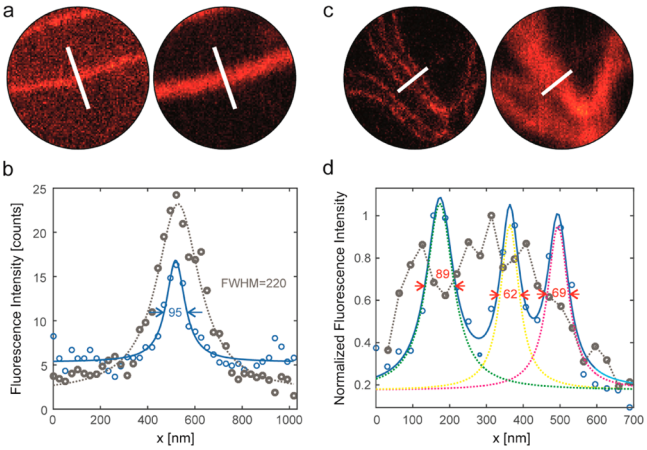


**Figure 5.** Line profiles in STED and confocal images of monoclonal vimentin-SNAP expressing U2OS cells, double stained with *610CP*-tubulin2 (a, b) and *680SiR*-SNAP probes (c, d; see Figure 6 for full images). (a, c) Confocal (right), STED (left) images, and (b, d) the corresponding line profiles: confocal (gray) and STED (blue). Lorentzian fits give full widths at half maxima (fwhm). (b) *610CP*-tubulin2 probe: confocal fwhm = 220 nm, STED fwhm = 95 nm. (d) *680SiR*-SNAP labeled vimentin filaments with a STED profile as a superposition of three Lorentzian fits (green, yellow and magenta), fwhm = 89, 62, and 69 nm, respectively.

was no more than 2-fold for *680SiR* and *SiR700*-$C_8$ SNAP tag ligands (cf. 7-fold response of *SiR*[8] even in the presence of high protein background; see Figure S4).

For two-color confocal and STED imaging, a blue-shifted dye can be chosen from cell membrane permeable fluorophores absorbing around 610−620 nm to ensure minimal crosstalk and clear color separation while maintaining the STED light intensity as low as possible for sufficient resolution. Several dedicated STED dyes (*610CP*, *620CP*,[9] and a new dye *620SiR* in Figure 1) were utilized in single color confocal imaging of genome edited vimentin-Halo expressing cells (610 nm excitation, 630−660 nm detection; Figure S5). From these, *610CP* was the dye of our choice due to its superior brightness. A *610CP*-based probe, based on a cabazitaxel derivative[28,29] with an 8-aminooctanoic acid linker,[13] was prepared and used for staining the native microtubule cytoskeleton in vimentin-SNAP expressing cells (Figure S6). The cell-to-cell reproducibility of two-color staining was verified by confocal microscopy. U2OS cells stably expressing vimentin-SNAP fusion proteins were incubated with *610CP*-tubulin2 (final concentration 5 $\mu$M) to label the microtubule cytoskeleton and *680SiR*-SNAP (final concentration 1 $\mu$M) for 60 min, washed for 60 min, and finally imaged using a Leica TCS SP8 beam scanning confocal microscope (Figure 4). In a control experiment, vimentin-SNAP was labeled in the same cells with 1 $\mu$M of either *680SiR*-SNAP or *SiR700*-$C_8$-SNAP probe and imaged under identical conditions, demonstrating superior brightness of the *680SiR*-derived probe in confocal images on this commercial setup (Figure S7).

For STED imaging, the cells were incubated first with *680SiR*-SNAP and then with *610CP*-tubulin2 probes (Figure 1), washed, and imaged in the two color STED microscope (for

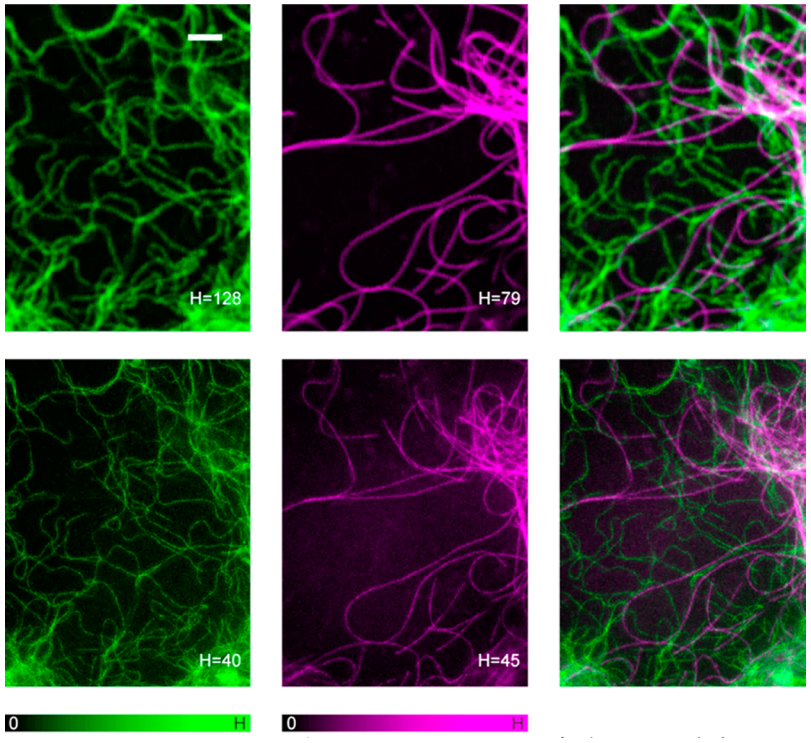


**Figure 6.** Two-color images of monoclonal vimentin-SNAP expressing U2OS cells, double stained with *680SiR*-SNAP and *610CP*-tubulin2 (for imaging scheme, see Figure S7). Upper row, left to right: confocal images of vimentin-SNAP stained with *680SiR*-SNAP (excitation: 676/10 nm, 6 $\mu$W, 732/68 nm detection), microtubule cytoskeleton stained with *610CP*-tubulin2 (excitation: 600/20 nm, 6 $\mu$W, detection: 645/30 nm), merge of vimentin (green) and tubulin (magenta) images. Lower row, left to right: the corresponding STED images. Color encodes the number of photons at each pixel. Switching between two excitation wavelengths was done pixelwise. Confocal images were recorded after the STED images. Pixel size: 25 nm. Pixel dwell time: 12 $\mu$s for 600 nm excitation and 16 $\mu$s for 676 nm excitation. STED wavelength: 810 nm, STED power: 100 mW. Scale bar: 2 $\mu$m.



DOI: 10.1021/acschembio.7b00616
*ACS Chem. Biol.* 2018, 13, 475−480

details, see Supporting Information). Figure 5 shows the data on optical resolution achieved in two color channels (defined in Figure S8). With *610CP*-tubulin2 and *680SiR*-SNAP probes, the apparent optical resolution values were found to be ca. 100 and 70 nm, respectively. The better optical resolution observed with dye *680SiR* is not surprising because of its much higher depletion efficiency at 810 nm as compared to *610CP*. While in the previous implementation of 810 nm NIR STED with *SiR* and *SiR700* dyes,[13] insufficient separation of the emission bands of the two dyes resulted in noticeable cross-talk between the detection channels necessitating an image subtraction procedure for clear color separation, no observable cross-talk between two color channels was detected with *680SiR* (see Figure 6).

**Conclusion.** We designed, engineered, and fully described here an 810 nm NIR STED setup for biology-related microscopy, implementing the longest STED wavelength reported so far. The new far-red-emitting cell-permeant silicon-rhodamine dye *680SiR*, tailored to this system, demonstrated high brightness and good imaging performance and is comparable and complementary to the earlier reported *SiR700* dye.[13] The observed difference between the excited state lifetimes of *680SiR* and *SiR700* is 1.6 ns, while several tenths of a nanosecond were shown to be sufficient for successful implementation of the multicolor fluorescence lifetime imaging (FLIM) method.[27] Therefore, we expect that this pair of dyes will fit the two-color NIR FLIM imaging scheme applicable to fluorophores indistinguishable only on the basis of their emission spectra. For the two-color STED imaging scheme implementing two excitation wavelengths and two detection windows (Figure S7), fluorescent dye *610CP* was identified as the complementary fluorophore demonstrating virtually no crosstalk with *680SiR*.

In our study, we demonstrated the use of the CRISPR/Cas9 method for endogenous tagging of a protein of interest combined with a newly established pair of NIR STED labels (*610CP* and *680SiR*). This approach provides stable expression of the fusion protein and therefore offers reliable and cell-to-cell reproducible dual-color nanoscale imaging in living cells.

## METHODS

**Fluorescence Microscopy.** Confocal imaging with dyes *610CP* and *680SiR* was performed on a Leica SP8 (Leica Microsystems, Mannheim, Germany) inverted confocal microscope equipped with an HC PL APO CS2 63x/1.40 OIL objective. Images were acquired using a 700 Hz bidirectional scanner, a pixel size of 70 × 70 nm, a pinhole of 95.6 $\mu$m (1 AU), and a frame averaging of 2.

The Supporting Information contains absorption and emission spectra of the new dyes (*620SiR* and *680SiR*); the data on the equilibrium between the zwitterionic (fluorescent) and spirolactone (nonfluorescent) forms of the dyes *680SiR* and *SiR* ($D_{0.5}$ values); fluorogenic response of *680SiR*-, *SiR700*-$C_8$-, and *SiR*-SNAP ligands to SNAP-tag protein; generation of knock-in cell lines; labeling of living cells; full descriptions of 810 nm STED setup; and the synthesis of dyes and their conjugates.

## ASSOCIATED CONTENT

### Supporting Information

The Supporting Information is available free of charge on the ACS Publications website at DOI: 10.1021/acschembio.7b00616.

Synthesis, purification, and characterization data for the dyes *620SiR* and *680SiR* and the ligands *680SiR*-SNAP, *SiR700*-$C_8$-SNAP, *620SiR*-Halo, and *610CP*-tubulin2; 810 nm STED setup description; procedure for generation of knock-in cell lines; Figures S1−S8 (PDF)

## AUTHOR INFORMATION


### Corresponding Authors

*E-mail: sjakobs@gwdg.de.
*E-mail: vbelov@gwdg.de.
*E-mail: shell@gwdg.de.

### ORCID

Vladimir N. Belov: 0000-0002-7741-4653
Stefan W. Hell: 0000-0002-9638-5077

### Present Address

[§]Department of Cell and Molecular Biology, Karolinska Institutet, SE-17177 Stockholm, Sweden

### Author Contributions

[‖]These authors contributed equally.



### Funding

The authors acknowledge the financial support provided by the German Bundesministerium für Bildung und Forschung (grant FKZ 13N14122).

### Notes

The authors declare no competing financial interest.

## ACKNOWLEDGMENTS

The authors are grateful to J. Bienert (MPI BPC Göttingen), H. Frauendorf (Georg-August-Universität Göttingen) and his co-workers for recording spectra, and J. Schimpfhauser (MPI BPC Göttingen) for the synthesis of the *610CP*-tubulin2 probe. Highly appreciated is the assistance of T. Gilat (MPI BPC Göttingen) with cell culturing and transfection.


## REFERENCES


(1) Hein, B., Willig, K. I., Wurm, C. A., Westphal, V., Jakobs, S., and Hell, S. W. (2010) Stimulated emission depletion nanoscopy of living cells using SNAP-tag fusion proteins. *Biophys. J. 98*, 158−163.

(2) Gibson, T. J., Seiler, M., and Veitia, R. A. (2013) The transience of transient overexpression. *Nat. Methods 10*, 715−721.

(3) Doudna, J. A., and Charpentier, E. (2014) The new frontier of genome engineering with CRISPR-Cas9. *Science 346*, 1258096.

(4) Wright, A. V., Nunez, J. K., and Doudna, J. A. (2016) Biology and Applications of CRISPR Systems: Harnessing Nature's Toolbox for Genome Engineering. *Cell 164*, 29−44.

(5) Ratz, M., Testa, I., Hell, S. W., and Jakobs, S. (2015) CRISPR/Cas9-mediated endogenous protein tagging for RESOLFT super-resolution microscopy of living human cells. *Sci. Rep. 5*, 9592.

(6) Wäldchen, S., Lehmann, J., Klein, T., van de Linde, S., and Sauer, M. (2015) Light-induced cell damage in live-cell super-resolution microscopy. *Sci. Rep. 5*, 15348.

(7) Pellett, P. A., Sun, X., Gould, T. J., Rothman, J. E., Xu, M.-Q., Corrêa, I. R., and Bewersdorf, J. (2011) Two-color STED microscopy in living cells. *Biomed. Opt. Express 2*, 2364−2371.

(8) Lukinavičius, G., Umezawa, K., Olivier, N., Honigmann, A., Yang, G., Plass, T., Mueller, V., Reymond, L., Corrêa, I. R., Jr., Luo, Z.-G., Schultz, C., Lemke, E. A., Heppenstall, P., Eggeling, C., Manley, S., and Johnsson, K. (2013) A near-infrared fluorophore for live-cell super-resolution microscopy of cellular proteins. *Nat. Chem. 5*, 132−139.

(9) Butkevich, A. N., Mitronova, G. Y., Sidenstein, S. C., Klocke, J. L., Kamin, D., Meineke, D. N. H., D'Este, E., Kraemer, P. T., Danzl, J. G., Belov, V. N., and Hell, S. W. (2016) Fluorescent rhodamines and fluorogenic carbopyronines for super-resolution STED microscopy in living cells. *Angew. Chem., Int. Ed. 55*, 3290−3294. ; *Angew. Chem. 2016, 128*, 3350−3355.

(10) Bottanelli, F., Kromann, E. B., Allgeyer, E. S., Erdmann, R. S., Wood Baguley, S., Sirinakis, G., Schepartz, A., Baddeley, D., Toomre,




DOI: 10.1021/acschembio.7b00616
*ACS Chem. Biol.* 2018, 13, 475−480

D. K., Rothman, J. E., and Bewersdorf, J. (2016) Two-colour live-cell nanoscale imaging of intracellular targets. *Nat. Commun. 7*, 10778.
(11) Sidenstein, S. C., D'Este, E., Böhm, M. J., Danzl, J. G., Belov, V. N., and Hell, S. W. (2016) Multicolour multilevel STED nanoscopy of actin/spectrin organization at synapses. *Sci. Rep. 6*, 26725.
(12) Hanne, J., Göttfert, F., Schimer, J., Anders-Össwein, M., Konvalinka, J., Engelhardt, J., Müller, B., Hell, S. W., and Kräusslich, H.-G. (2016) Stimulated emission depletion nanoscopy reveals time-course of human immunodeficiency virus proteolytic maturation. *ACS Nano 10*, 8215−8222.
(13) Lukinavičius, G., Reymond, L., Umezawa, K., Sallin, O., D'Este, E., Göttfert, F., Ta, H., Hell, S. W., Urano, Y., and Johnsson, K. (2016) Fluorogenic probes for multicolor imaging in living cells. *J. Am. Chem. Soc. 138*, 9365−9368.
(14) Mourant, J. R., Fuselier, T., Boyer, J., Johnson, T. M., and Bigio, I. J. (1997) Predictions and measurements of scattering and absorption over broad wavelength ranges in tissue phantoms. *Appl. Opt. 36*, 949−957.
(15) Escobedo, J. O., Rusin, O., Lim, S., and Strongin, R. M. (2010) NIR dyes for bioimaging applications. *Curr. Opin. Chem. Biol. 14*, 64−70.
(16) Renikuntla, B. R., Rose, H. C., Eldo, J., Waggoner, A. S., and Armitage, B. A. (2004) Improved photostability and fluorescence properties through polyfluorination of a cyanine dye. *Org. Lett. 6*, 909−912.
(17) Ormond, A. B., and Freeman, H. S. (2013) Dye sensitizers for photodynamic therapy. *Materials 6*, 817−840.
(18) Hu, L., Yan, Z., and Xu, H. (2013) Advances in synthesis and application of near-infrared absorbing squaraine dyes. *RSC Adv. 3*, 7667−7676.
(19) Koide, Y., Urano, Y., Hanaoka, K., Piao, W., Kusakabe, M., Saito, N., Terai, T., Okabe, T., and Nagano, T. (2012) Development of NIR fluorescent dyes based on Si-rhodamine for in vivo imaging. *J. Am. Chem. Soc. 134*, 5029−5031.
(20) Butkevich, A. N., Belov, V. N., Kolmakov, K., Sokolov, V. V., Shojaei, H., Sidenstein, S. C., Kamin, D., Matthias, J., Vlijm, R., Engelhardt, J., and Hell, S. W. (2017) Hydroxylated Fluorescent Dyes for Live-Cell Labeling: Synthesis, Spectra and Super-Resolution STED Microscopy. *Chem. - Eur. J. 23*, 12114−12119.
(21) Liu, J., Sun, Y.-Q., Zhang, H., Shi, H., Shi, Y., and Guo, W. (2016) A photostable near-infrared fluorescent tracker with pH-independent specificity to lysosomes for long time and multicolor imaging. *ACS Appl. Mater. Interfaces 8*, 22953−22962.
(22) Zhou, X., Lai, R., Beck, J. R., Li, H., and Stains, C. I. (2016) Nebraska Red: a phosphinate based near-infared fluorophore scaffols for chemical biology applications. *Chem. Commun. 52*, 12290−12293.
(23) Grimm, J. B., English, B. P., Chen, J., Slaughter, J. P., Zhang, Z., Revyakin, A., Patel, R., Macklin, J. J., Normanno, D., Singer, R. H., Lionnet, T., and Lavis, L. D. (2015) A general method to improve fluorophores for live-cell and single molecule microscopy. *Nat. Methods 12*, 244−250.
(24) Zhang, X.-F., Zhang, Y., and Liu, L. (2014) Fluorescence lifetimes and quantum yields of ten rhodamine derivatives: structural effect on emission mechanism in different solvents. *J. Lumin. 145*, 448−453.
(25) Grimm, J. B., Klein, T., Kopek, B. G., Shtengel, G., Hess, H. F., Sauer, M., and Lavis, L. D. (2016) Synthesis of a far-red photoactivatable silicon-containing rhodamine for super-resolution microscopy. *Angew. Chem., Int. Ed. 55*, 1723. ; *Angew. Chem.* 2016, *128*, 1755−1759.
(26) Kozma, E., Estrada Girona, G., Paci, G., Lemke, E. A., and Kele, P. (2017) Bioorthogonal double-fluorogenic siliconrhodamine probes for intracellular super-resolution microscopy. *Chem. Commun. 53*, 6696−6699.
(27) Niehörster, T., Löschberger, A., Gregor, I., Krämer, B., Rahn, H.-J., Patting, M., Koberling, F., Enderlein, J., and Sauer, M. (2016) Multi-target spectrally resolved fluorescence lifetime imaging microscopy. *Nat. Methods 13*, 257−262.
(28) Morley, S. J., Qi, Y., Iovino, L., Andolfi, L., Guo, D., Kalebic, N., Castaldi, L., Tischer, C., Portulano, C., Bolasco, G., Shirlekar, K., Fusco, C. M., Asaro, A., Fermani, F., Sundukova, M., Matti, U., Reymond, L., De Ninno, A., Businaro, L., Johnsson, K., Lazzarino, M., Ries, J., Schwab, Y., Hu, J., and Heppenstall, P. A. (2016) Acetylated tubulin is essential for touch sensation in mice. *eLife 5*, e20813.
(29) Wang, Y., Feng, F., Chen, L., Zhao, H., and Tian, L. (2014) Isolation, identification and characterization of potential impurities in cabazitaxel and their formation. *Magn. Reson. Chem. 52*, 783−788.


DOI: 10.1021/acschembio.7b00616
*ACS Chem. Biol.* 2018, 13, 475−480